

Synthesis of $CaxCu_{3-x}Ti_4O_{12}$ Perovskite Materials and house-hold LED light mediated degradation of Rhodamine Blue dye

Priyankamoni Saikia

Tezpur University

Hemanga Jyoti Sarmah

Tezpur University

Shahnaz Ahmed

Tezpur University

Suman Lahkar

Tezpur University

Jyoti Prakash Das

Tezpur University

Swapan Kumar Dolui (✉ dolui@tezu.ernet.in)

Tezpur University

Original Research Full Papers

Keywords: Perovskite, Photocatalyst, Dye degradation, Calcium Copper Titanate, LED light

Posted Date: February 3rd, 2021

DOI: <https://doi.org/10.21203/rs.3.rs-190338/v1>

License: © ⓘ This work is licensed under a Creative Commons Attribution 4.0 International License.

[Read Full License](#)

Version of Record: A version of this preprint was published at Journal of Inorganic and Organometallic Polymers and Materials on February 22nd, 2021. See the published version at <https://doi.org/10.1007/s10904-021-01929-y>.

1 **Synthesis of $\text{Ca}_x\text{Cu}_{3-x}\text{Ti}_4\text{O}_{12}$ Perovskite Materials and house-hold LED light**
2 **mediated degradation of Rhodamine Blue dye**

3 Priyankamoni Saikia¹, Hemanga Jyoti Sarmah², Shahnaz Ahmed¹, Suman Lahkar¹,
4 Jyoti Prakash Das¹ and Swapan Kumar Dolui^{1,*}

5 ¹*Department of Chemical Sciences, Tezpur University, Napaam, Tezpur, 784028, Assam,*
6 *India*

7 ²*Department of Physics, Tezpur University, Napaam, Tezpur, 784028, Assam, India*

8 Corresponding author, Email ID: dolui@tezu.ernet.in , priyankam@tezu.ernet.in.

9

10

11

12

13

14

15

16

17

18

19

20

1 **ABSTRACT:** This report describes a comparative study of dye degradation under 20-watt
2 LED light using the perovskite photocatalyst Calcium Copper Titanate (CCTO) and its
3 compositions ($\text{Ca}_x\text{Cu}_{3-x}\text{Ti}_4\text{O}_{12}$) ($x=1, 1.5$ and 2), synthesized by changing molar ratios of Ca^{2+}
4 and Cu^{2+} ions. The 99.74% degradation of Rhodamine Blue (RhB) with composition ($x=1$)
5 within 6 h is reflected its better photocatalytic activity than the parent CCTO and other
6 compositions. The band gap energy of the materials 2.18 eV (CCTO), 1.93 eV ($x=1$), 2.40 eV
7 ($x=1.5$), and 2.55 eV ($x=2$) are analysed with UV-Vis spectroscopy. The presences of Ca, Cu,
8 Ti and O in the synthesized photocatalysts are confirmed with Elemental X-ray Dispersive
9 (EDX) analysis. The cubic phases in the polyhedral shape of the materials are detected in X-
10 ray diffraction and Scanning Electron Microscopy (SEM). This report further observes the
11 defect density concentrations of the materials with Photoluminescence Spectroscopy (PL) and
12 provides the approximate explanation of their dye degradation performance as photocatalysts.
13 The rate constants are found in a first order reaction trend; where the composition ($x=1$)
14 shows about $1.683 \times 10^{-2} \text{ min}^{-1}$. The mechanistic understanding of the degradation process is
15 also revisited and rationalized with different scavengers for the process.

16 **Keywords:** *Perovskite, Photocatalyst, Dye degradation, Calcium Copper Titanate, LED*
17 *light*

18 **1. Introduction**

19 As we are shifting towards modernization, there is a rapid development of industrialization
20 and urbanization which ultimately affects the ecosystem by discharging toxic elements and
21 pollutants into the natural water cycle [1,2]. The treatment of wastewater is essential to
22 maintain not only for a pollutant-free ecosystem of aquatic system, but also for a sustainable
23 environment to the all living system [3-5]. As a part of waste management system, finding a
24 sustainable approach to degrade the toxic pollutants is very urgent responsibility for both

1 small companies and big industries. Recently, the oxidation process by semiconductor-based
2 photocatalyst has emerged as one of the potential fields from sustainable chemistry. The
3 degradation process of the pollutants requires an active photocatalyst which can be excited by
4 the photons and generate electrons and holes which ultimately able to reduce the pollutants
5 [6-9]. Among the various photocatalyst; TiO_2 , CdS , ZnO , WO_3 etc. are extensively used in
6 wastewater treatment [10-13]. Still there are some challenges for the catalysis process,
7 because of larger band gap of the aforementioned catalysts. TiO_2 have a band gap of 3.2 eV
8 and the material need UV region to show photocatalytic activity. Since ordinary sunlight
9 contains only 5% UV light, making TiO_2 quite less effective in the degradation process under
10 sunlight condition [14]. The development of a photocatalyst having a narrow bandgap is one
11 of the crucial properties where visible light can be used in the degradation process. Moreover,
12 the previously discussed materials have a high rate of recombination of electrons and holes,
13 which limits their uses in the long run.

14 Among the various kinds of light active photocatalyst, the perovskite-based
15 photocatalyst has a unique photophysical property due to its distinct advantages [15-19]
16 Perovskite compounds such as BaTiO_3 [20], CaTiO_3 [21], CoTiO_3 [22], NiTiO_3 [23], LaFeO_3
17 [24] are extensively used as a photocatalyst due to its favourable band edge properties.

18 In the family of perovskite photocatalyst, Calcium Copper Titanate (CCTO) has
19 gained much attention as a cubic double perovskite which shows a good photocatalytic
20 reaction against water pollutants and pharmaceutical wastes [25,26]. In crystallographic
21 analysis, CCTO appears in ideal cubic structure of BBC lattice, bearing a space group of $\text{Im}\bar{3}$,
22 where *A* site is shared by two ions that are Ca^{2+} and Cu^{2+} and the *B* site is shared by Ti^{4+} ions
23 [15]. Due to the difference in ionic radii tilting of the TiO_6 octahedral plane maybe observed
24 [27,28]. As TiO_2 is a UV active photocatalyst and CuO is a visible light active photocatalyst,
25 it was seen that an effective combination of these compounds makes CCTO a visible light

1 active photocatalyst. In the past two decades, CCTO material has been widely investigated
2 for their various physical properties and applications [29,30]. The cationic substitution and its
3 concentration in CCTO material can largely manifest the photocatalytic activity [31]. CCTO
4 material can be synthesized by two major methods one is a high-temperature solid-state
5 method [26] another is a wet chemistry method [31]. The solid-state method has some
6 disadvantages in maintaining the purity as the synthesised materials contain some impurities
7 such as CaTiO_3 and CuO etc. [32,33]. To resolve these disadvantages, the alternative
8 developed methodologies are the wet chemistry method including polymerized complex
9 [34,35], microwave dealing [36], sol-gel [33], co-precipitation method [37] and many more.
10 Degradation of harmful dyes by CCTO have been reported by different groups [17,38,39].
11 Otitoju et. al. studied the degradation of Rhodamine Blue (RhB) in the presence of
12 $\text{CaCu}_3\text{Ti}_4\text{O}_{12}$ modified polyethersulfone fibre membrane. [18]. Zhu and his co-workers
13 studied the removal of ibuprofen in presence of CCTO catalyst under visible light irradiation
14 [39]. Kushwaha's group studied the photocatalytic property of a composite of polyaniline and
15 CCTO in the degradation of congo red and methyl orange under the illumination of a visible
16 light source [17].

17 Though, degradation of harmful dyes by CCTO catalyst have been reported, but proper
18 correlation of degradation with the defect density of the specimen have not addressed in the
19 literature. Here, we synthesize of the CCTO and its compositions ($\text{Ca}_x\text{Cu}_{3-x}\text{Ti}_4\text{O}_{12}$, where
20 $x=1, 1.5, 2$) by citrate precursor method with varying the molar ratios of Ca^{2+} and Cu^{2+} and
21 the materials can be used for dye-degradation of Rhodamine Blue under user-friendly
22 household 20-watt LED light. Surprisingly, the degradation of RhB is found better using
23 composition of $x=1$ than the parent CCTO and other compositions. The photoluminescence
24 (PL) properties of all materials are studied and the defect density calculations are explained.
25 The catalyst $\text{Ca}_x\text{Cu}_{3-x}\text{Ti}_4\text{O}_{12}$, ($x=1$) have shown a promising result with 99.74 % degradation,

1 within 6 h. Additionally, the observed degradation efficiency of the synthesized materials and
2 rate constants of the photocatalytic processes are studied with comparison of defect density
3 concentrations calculated by PL studies.

4 **2. Experimental Section**

5 **2.1. Materials**

6 Calcium carbonate, CaCO_3 (98.5% Avantor), copper chloride dihydrate, $\text{CuCl}_2 \cdot 2\text{H}_2\text{O}$ (99.0%
7 Merck), anhydrous citric acid, $\text{C}_6\text{H}_8\text{O}_7$ (99.0% Merck), titanium dioxide, TiO_2 (98.5%
8 Merck) were purchased from commercial source and used a starting material, without any
9 further purification.

10 **2.2. Methods**

11 Calcium Copper Titanate compositions were synthesized by conventional citrate precursor
12 method reported by Turkey et. al. [40]. CaCO_3 , TiO_2 , $\text{CuCl}_2 \cdot 2\text{H}_2\text{O}$, and citric acid $\text{C}_6\text{H}_8\text{O}_7$ was
13 taken as a raw material. To prepare CCTO ($\text{CaCu}_3\text{Ti}_4\text{O}_{12}$), the aqueous solution of CaCO_3 ,
14 $\text{CuCl}_2 \cdot 2\text{H}_2\text{O}$, and TiO_2 were mixed in molar ratio 1:3:4 respectively. The certain amount of
15 Citric acid was also taken which acts as a complexing agent. The molar ratio of metal
16 precursor to the citric acid is the amount of is 1:5. The obtained light-coloured solution was
17 slowly heated at 80 °C to form a gel. Subsequently, the gel was calcinated at 1000 °C for 2
18 hours at a heating rate of 10 °C/min in a muffle furnace to achieve the target material
19 $\text{CaCu}_3\text{Ti}_4\text{O}_{12}$ in perovskite structure. To prepare the CCTO derived material in various
20 compositions, the above-mentioned compounds are now mixed in the different ratio of x:3-
21 x:4 where x=1, 1.5 and 2. The synthesized materials are named as CCTO (x=1), CCTO
22 (x=1.5) and CCTO (x=2) respectively.

1 **2.3. Characterization**

2 To find the structural analysis, X-ray Diffraction (XRD) studies were carried using Rigaku
3 Miniflex X-ray diffractometer (Tokyo, Japan), equipped with $\text{CuK}\alpha$ radiation ($\lambda = 0.15418$
4 nm, scanning rate = 0.05 s^{-1}) at 30 kV and 15 mA; where data is acquired in the 2θ range of
5 7° to 80° . In addition, The FTIR spectra of the samples were recorded with a Nicolet Impact-
6 410 IR spectrometer (USA) in the KBr medium at room temperature in the range of 4000–
7 400 cm^{-1} , to have a proper understanding of IR active bonds present in the host system. In
8 optical studies, absorption and emission spectra were acquired using a Shimadzu UV-2550
9 and Hitachi F-2700 fluorescence spectrophotometer respectively. For morphological and
10 elemental analysis, we employed Scanning electron Microscope (SEM) and elemental
11 dispersive X-ray analysis technique (JEOL-JSM-6390LV). Additionally, the surface area and
12 pore size of the material was evaluated by Brunauer Emmett-Teller (BET) using a BET
13 analyser (Model 1000E, Quantachrome, USA).

14 **2.4. Photodegradation Procedure**

15 Light emitting diodes (LED) have many advantages like low consumption energy, long-
16 lasting life, and narrow-spectrum luminescence properties, etc. In this study, we have used a
17 domestic visible LED light of 20 W (Philips LED lamp B22, 2000 lumen) which was placed
18 at a distance of 8 cm just above the reaction vessel. The whole system was enclosed by a
19 cardboard box of dimensions $44 \times 35 \times 36.5 \text{ cm}^3$ (Length \times Width \times Height). The reaction was
20 carried out at a temperature of $30 \pm 5 \text{ }^\circ\text{C}$; where, monitoring was carried out by an ordinary
21 thermometer. Rhodamine Blue (RhB) stock solution was prepared in distilled water at a
22 concentration of 100 ppm. Photodegradation of RhB dye solution was monitored by a
23 Shimadzu UV-2550 spectrophotometer using a path length of $\sim 1 \text{ cm}$. For the photocatalytic
24 experiment, 50 mg of catalyst was added to a 5 mL (100 ppm) dye stock solution which was

1 diluted by 95 mL H₂O and 1 mL H₂O₂ and stirred in dark for 12 hours to attain the
2 adsorption/desorption equilibrium. LED was switched on to start the experiment which was
3 continued for optimized hours. At a certain interval, 5 mL of the sample was taken out from
4 the reactor, centrifuged it and the dye content in the solution was analysed through absorption
5 spectroscopy.

6 **3. Results and discussion**

7 **3.1. Powder X-ray diffraction**

8 As a part of structural analysis, Powder XRD technique was carried out for CCTO and its
9 compositions (x=1, 1.5, 2), the diffraction pattern was showed in the (ESI, Fig S1). The
10 diffraction peaks (220), (400), (422) planes was observed, which essentially corresponds to
11 the cubic phase of CCTO, in accordance to the JCPDS No. 75-2188 [40]. Some secondary
12 weak diffraction peaks were also observed which is due to the noise or impurities like CuO
13 and TiO₂ [40]. Knowing the cubic phase of the material, the lattice parameter and the unit cell
14 volume for the specimen were calculated by using the following equations [41].

$$15 \quad d_{hkl} = \frac{a}{\sqrt{h^2+k^2+l^2}} \quad (1)$$

$$16 \quad V_{\text{cell}} = a^3 \quad (2)$$

17 The degree of crystallinity can be estimated by the following relation [42].

$$18 \quad \text{Crystallinity} = \frac{\text{Area of crystallite peak}}{\text{Area of all peaks}} \quad (3)$$

19 The average crystallite size was calculated using the Debye Scherrer formula [43].

$$20 \quad D = \frac{0.9\lambda}{B\cos\theta} \quad (4)$$

1 where D and λ are defined as the crystallite size and the wavelength of $CuK\alpha$
 2 radiation. And, 2θ and B are defined as peak position and the full width half maximum
 3 (FWHM) in radians respectively. The variations in structural parameters are depicted in the
 4 Table 1.

5 **Table 1. Structural parameters of produced Calcium Copper Titanate (CCTO) and its**
 6 **compositions (x=1, 1.5, 2).**

CCTO Compositions	Volume of unit cell (cm^{-3})	Crystallinity (%)	Crystallite size (nm)
CCTO	0.433333	8.48	22.0
CCTO (x=1)	0.396133	10.6	21.1
CCTO (x=1.5)	0.394767	8.51	16.7
CCTO (x=2)	0.40135	8.48	16.1

7

8 3.2. FT-IR Analysis

9 For identifying the IR active bonding information, the materials were studied with the FT-IR
 10 spectroscopy. The FT-IR spectra of CCTO and its compositions (x=1, 1.5, 2) was showed in
 11 Fig. S2 (ESI). The broad absorption peak at $\sim 3430 \text{ cm}^{-1}$ can be attributed for O-H stretching
 12 frequency [44]. Moreover, the absorption peak at $\sim 463 \text{ cm}^{-1}$ is responsible due to the Ti-O-Ti
 13 stretching frequency [45]. Furthermore, the Cu-O and Ca-O bending vibration can be
 14 identified from the peak at $\sim 525 \text{ cm}^{-1}$ at 606 cm^{-1} [45]. The evidence of an absorption band
 15 located at $380\text{-}700 \text{ cm}^{-1}$ can be considered due to the mixed vibrations of TiO_6 and CuO_4 [45].
 16 As the peak intensity of the Cu-O ($\sim 525 \text{ cm}^{-1}$) was gradually decreased from compositions
 17 x=1 to x=2, this implied that the copper content was decreasing from compositions x=1 to
 18 x=2.

1 **3.3. Morphological and elemental analysis**

2 The morphological characters in the CCTO derivatives were analysed using scanning
3 electron microscopy. The SEM images of the CCTO derivatives can be observed in Fig. S3
4 (ESI). As noticed from the image that the synthesised material was observed in polyhedral
5 shapes. These shapes maybe approximated to a cubic morphology. Further analysis
6 confirmed that particle have size in the range of 1 μm . The different calculated sizes of
7 particles were embedded in the same figure. It is well known that, polyhedral shape of
8 materials is a better candidate for the photocatalytic activity, so our synthesised material
9 possibly show a better activity as photocatalyst [19,46]. Further analysis on those images
10 ensured us the presence of large microstructure matrix where small grains were ingrained in
11 between the large grains.

12 The elemental information of the synthesized materials were analysed with Energy
13 Dispersive X-Ray Spectrum (EDX) technique for CCTO specimen. EDX spectra of the
14 materials were shown in the Fig. S4 (ESI). The presence of Ca, Cu, Ti and O in the host
15 material was observed in the image. Different concentration of the elements was presented in
16 the upper inset of the same figure.

17 **3.4. Absorption and emission Spectroscopy**

18 The optical properties, both absorption and emission responses were studied. For absorption
19 studies, UV-Vis spectra were carried out in the range 200 to 800 nm. The band gap energy of
20 the specimen under study was estimated using the Tauc plot from derived absorption data. A
21 straight-line can be drawn in order to estimate the band gap of the system, in accordance to
22 the Tauc relation [40]

$$23 \quad (\alpha h\nu)^m = h\nu - E_g \quad (5)$$

1 where α is the optical absorption co-efficient, h is the Planck's constant, ν is the Photon's
2 frequency, E_g is the bandgap energy [40] and m is a constant associated with a different type
3 of transitions ($m=1/2$ to indirect transitions and $m= 2$ for direct transitions) [47]. In this case,
4 we have considered the optical transitions as a result of allowed direct band to band
5 transition. For CCTO, CCTO ($x=1$), CCTO ($x=1.5$), and CCTO ($x=2$) (with different ratios of
6 Ca and Cu ions the band gap energy was estimated to 2.18, 1.93, 2.40, and 2.55 eV
7 respectively (ESI, Fig S5). Moreover, due to incorporations of Cu or Ca in the CCTO lattice
8 caused the distortions in between TiO_6 and CaO leading to the appearing of some
9 intermediate levels in between the valence band and conduction band [40,48].

10 The photoluminescent (PL) emission Spectra of $Ca_xCu_{3-x}Ti_4O_{12}$ were studied and presented
11 in the Fig S6 (ESI). The excitation peak for the luminescent spectra was fixed on the band
12 gap of the respective specime. We observed an asymmetric and broad spectra, implying
13 presence of surface or defect states in the host system [49]. A deconvoluted spectra could be
14 seen in the Fig. S6 (ESI). Upon deconvolution, we observed multiple peaks, for a band gap
15 excitation. The first peak appearing near the band gap, maybe assigned for the near band edge
16 emission. At the same time, other peaks could be associated with the defective origin, which
17 usually appear in forbidden region. The defect density of the system was estimated by
18 measuring the integral intensity (area under the curve) of the second peak, compared to the
19 NBE peak. Theoretically, the integral intensity for a defective peak qualitatively represents
20 better defect concentration in the system. We observed large integral intensity of defective
21 peak with respect to NBE. for CCTO ($x=1$) compared to the other samples, implying highest
22 defect concentration. This maybe responsible for better photocatalytic activity of the specimen
23 under study.

24

1 **Table 3: Comparison of defect density of different compositions of the photocatalyst.**

2	Photocatalyst	The integral intensity of the defective peak
3	CCTO	1.2086
4	CCTO (x=1)	1.454
5	CCTO (x=1.5)	1.382
6	CCTO (x=2)	1.227

7 **3.5. Photocatalytic activity**

8 To start the study the photo-catalysis activity of the prepared catalyst, we selected 20-Watt
9 LED bulb as a light source, and Rhodamine dye (RhB) as a standard pollutant. Prior to the
10 irradiation and catalyst addition, the UV-Vis spectroscopy of the prepared Rhodamine Blue
11 (RhB) stock solution was checked and observed a noticeable absorption peak at 552 nm. The
12 prepared catalyst were added to the solution and allowed for rigorous stirring for a period of
13 12 h to achieve adsorption-desorption equilibrium. Upon exposure to the LED light, we
14 observed a clear drop in the absorption value of the spectra, merely signifying the
15 degradation process (ESI, Fig S7). To be noted, in UV-Vis spectroscopy, the intensity of
16 absorption depends on the amount of concentration; thus, declining trend of the absorption
17 intensity confirms the degradation of the same. Degradation of RhB was achieved us using all
18 the prepared catalyst, can be seen in the Fig. S7 (ESI). After illumination for 6 h, we noticed
19 degradation efficiency to a value of 87 %, 99.7 %, 75 %, 85 % and for CCTO, CCTO (x=1),
20 CCTO (x=1.5) and CCTO (x=2) respectively. The prepared catalyst CCTO (x=1) exhibited a
21 better performance as photo-catalyst.

22

1 The degradation percentage of Rhodamine blue was calculated by using the following
2 equation [50]:

$$3 \quad \text{Degradation rate } (r) = \frac{C_0 - C}{C_0} \times 100\% \quad (6)$$

4 Where, C_0 and C are the concentration of Rhodamine Blue solution at $t=0$ (initial), and any
5 time t , respectively [50]. As the absorption in UV-Vis spectra depends on the concentration,
6 so the equation (6) maybe re-write in terms of absorbance, A_0 (initial) and A (any time t) as:

$$7 \quad r = \frac{A_0 - A}{A_0} \times 100\% \quad (7)$$

8 Moreover, the kinetics of photocatalytic degradation of Rhodamine Blue was assumed to be
9 first order and reaction rate was determined by using the following Langmuir Hinselwood
10 kinetic equation

$$11 \quad \ln (C_0/C) = kt + \text{constant} \quad (8)$$

12 k is the first-order rate constant (unit is min^{-1}), which can be calculated from the slope of the
13 graph of $\ln (C_0/C)$ versus irradiate time t [38,50,51]. The photocatalytic performance of the
14 product of the different components of the ratio of Ca and Cu ions were compared in a typical
15 photocatalyst experiment were analyzed (ESI, Fig S8). The degradation observed using
16 CCTO was noticeable within first two hours, but it showed a saturation trend later. However,
17 CCTO ($x=1$) was found to show the most satisfactory result by degrading 99.74% in only 6 h.
18 While the other composite CCTO ($x=1.5$) and CCTO ($x=2$) showed only 78.85% and 99.95%
19 degradation respectively.

20

21

1 **Table 2: Comparison of degradation efficiency of different compositions of the**
 2 **photocatalyst**

Photocatalyst	Degradation percentage	Irradiation time (min)	Degradation rate constant(min^{-1})
CCTO	99.6%	1440	0.53×10^{-2}
CCTO (x=1)	99.74%	360	1.683×10^{-2}
CCTO (x=1.5)	78.85%	420	0.302×10^{-2}
CCTO (x=2)	99.95%	440	0.444×10^{-2}

3 The rate constant for CCTO (x=1) ($1.683 \times 10^{-2} \text{ min}^{-1}$) was found higher than that of the other
 4 three compositions which are attributed due to the higher defect density than that of the other
 5 compositions, which may be ensured from the PL studies. The defect density was increased
 6 initially, with varying x-value, before achieving saturation. When the material was changed
 7 from CCTO to composition x=1, the defect density was found improving, resulting an
 8 enhancement of reaction rate. Analysing the same for compositions x=1.5 and 2, the defect
 9 density was observed declination gradually. The rate constant was dropped in similar trend
 10 abruptly (at x=1.5), before getting saturated (Fig. S9 ESI). The comparison of the degradation
 11 efficiency and rate constants for different catalyst were shown in the Table 2. In our study,
 12 the best result was observed for (x=1) compositions, favouring a better degradation rate
 13 constant. The materials may be considered for waste water treatment.

14 **3.6. Surface Area Study.**

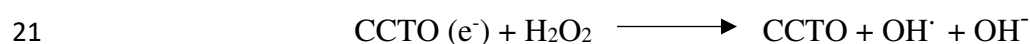
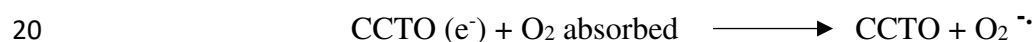
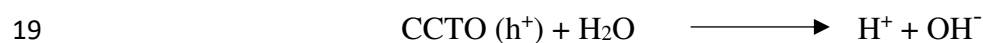
15 Brunauer Emmett-Teller (BET) was studied for the CCTO (x=1) specimen. The pore volume
 16 and surface area obtained by the specimen under study were 0.024 cc/g and 3.009 m^2/g
 17 respectively. The surface area of the material was high, which is a property of a good
 18 photocatalyst, and also large pore volume indicates the material as a good penetration of light

1 and contributing as an effective way of degrading the RhB dye [52]. The average pore radius
 2 is about 22.162 Å. The BET isotherm indicated that the material was exhibited a type-III
 3 isotherm (ESI, Fig S10).

4 **4. Mechanistic Insight**

5 To determine the active species in the degradation of Rhodamine Blue various scavenger test
 6 was done. Isopropanol was used to identify OH[•] scavenger and p-benzoquinone for O₂^{•-}
 7 radical scavenger. The degradation of Rhodamine Blue in the presence of various scavengers
 8 was highlighted (ESI, Fig S11). In addition to benzoquinone (BQ), the degradation process
 9 was suppressed which indicates that the main active species in the degradation process is
 10 superoxide anion (O₂^{•-}). When the visible light is irradiated on the surface of the CCTO
 11 catalyst, electrons and holes are generated (ESI, Fig S12). The number of holes generated in
 12 the valence band is the same as the number of electrons generated in the conduction band
 13 [52]. The electrons from the conduction band react with absorbed oxygen to generate reactive
 14 superoxide (O₂^{•-}) radical which further reacts with water to produce hydroxyl radical (OH[•]).
 15 On the other hand, holes in the valence band react with a water molecule to generate OH[•]
 16 radical [50].

17 The main reactions are given below





2 **5. Conclusion**

3 In summary, we have prepared a perovskite photocatalyst calcium copper titanate (CCTO)
4 and its compositions *via* the citrate precursor method. The prepared catalysts were observed
5 in polyhedral shape bearing a crystallographic cubic phase. The photocatalytic property of the
6 material was examined through the degradation of Rhodamine Blue dye under the
7 illumination of 20-Watt LED light. The efficiency of the degradation of the composition
8 CCTO (x=1) was excellent, having a degradation efficiency of 99.74% within 6 hours. The
9 kinetic studies of the degradation process with the composition x=1 also showed the higher
10 rate constant of the reaction in comparison to other synthesized materials. The PL study of
11 the materials justified the higher defect concentration and followed by its photocatalytic
12 performance. This simple 20-watt LED light driven protocol for photodegradation of dye
13 could be very useful for medium scale pollutant cleaning or might possible in large scale too.

14 **Funding**

15 The author has received research support from Tezpur University for providing the
16 Institutional Fellowship.

17 **Corresponding Author**

18 Correspondence to Prof. Swapan Kumar Dolui.

19 **Conflict of Interest**

20 The authors declare that they have no conflicts of interest.

21 **Author Contributions**

22 The manuscript was written through the contributions of all authors. All authors have
23 approved the final version of the manuscript.

1 **Acknowledgment**

2 The author would also like to thank the Sophisticated Analytical Instrumentation Centre
3 (SAIC), Tezpur University, India for providing analytical support.

4 **Reference**

- 5 [1] B. Lellis, C. Z. Fávaro-Polonio, J.A. Pamphile, J. C. Polonio, *Biotechnology Research*
6 *and Innovation*. **3**, 275-290 (2019)
- 7 [2] D. A. Yaseen, M. Scholz, *International journal of environmental science and*
8 *technology*. **16**, 1193-1226 (2019)
- 9 [3] S. Adhikari, A. V. Charanpahari, G. Madras, *ACS omega*. **10**, 6926-6938 (2017)
- 10 [4] C. Kulsi, A. Ghosh, A. Mondal, K. Kargupta, S. Ganguly, D. Banerjee, *Applied Surface*
11 *Science*, **392**, 540-548 (2017)
- 12 [5] C. Sarkar, C. Bora, S. K. Dolui, *Industrial & Engineering Chemistry Research*, **53**, 16148-
13 16155 (2014)
- 14 [6] A. Ghosh, M. Mitra, D. Banerjee, A. Mondal, *RSC advances*, **27**, 22803-22811 (2016)
- 15 [7] X. Li, J. Xie, C. Jiang, J. Yu, P. Zhang, *Frontiers of Environmental Science &*
16 *Engineering*, **12**, 14 (2018)
- 17 [8] S. Dong, J. Feng, M. Fan, Y. Pi, L. Hu, X. Han, M. Liu, J. Sun, J. Sun, *Rsc Advances*, **19**,
18 14610-14630 (2015)
- 19 [9] F. Opoku, K. K. Govender, C. G. C. E. van Sittert, P. P. Govender, *Advanced Sustainable*
20 *Systems*, **1**, 1700006 (2017)
- 21 [10] J. Yang, C. Chen, H. Ji, W. Ma, J. Zhao, *The Journal of Physical Chemistry B*, **109**,
22 21900-21907 (2005)

- 1 [11] B. Pan, Y. Xie, S. Zhang, L. Lv, W. Zhang, ACS applied materials & interfaces, **4**,
2 3938-3943 (2012)
- 3 [12] K.Intarasuwan, P. Amornpitoksuk, S. Suwanboon, P. Graidist, Separation and
4 Purification Technology, **177**, 304-312 (2017)
- 5 [13] X. Liu, H. Zhai, P. Wang, Q. Zhang, Z. Wang, Y. Liu, Y. Dai, B. Huang, X. Qin, X.
6 Zhang, Catalysis Science & Technology, **9**, 652-658 (2019)
- 7 [14] P. Magalhaes, L. Andrade, O. C. Nunes, A. Mendes, Reviews on Advanced Materials
8 Science, **51**, (2017)
- 9 [15] J. H. Clark, M. S. Dyer, R. G. Palgrave, C. P. Ireland, J. R. Darwent, J. B. Claridge, M.
10 J. Rosseinsky, Journal of the American Chemical Society, **133**, 1016-1032 (2011)
- 11 [16] A. Sen, K. K. Chattopadhyay, Journal of Materials Science: Materials in Electronics, **27**,
12 10393-10398 (2016)
- 13 [17] H. S. Kushwaha, P. Thomas, R. Vaish, RSC advances, **5**, 87241-87250 (2015)
- 14 [18] T. A. Otitoju, D. Jiang, Y. Ouyang, M. A. M. Elamin, S. Li, Journal of Industrial and
15 Engineering Chemistry, **83**, 145-152 (2020)
- 16 [19] P. Kanhere, Z. Chen, Molecules, **19**, 19995-20022 (2014)
- 17 [20] K.Maeda, ACS applied materials & interfaces, **6**, 2167-2173 (2014)
- 18 [21] H. Zhang, G. Chen, Y. Li, Y. Teng, International journal of hydrogen energy, **35**, 2713-
19 2716 (2010)
- 20 [22] Y. Qu, W. Zhou, H. Fu, ChemCatChem, **6**, 265-270 (2014)
- 21 [23] Y.Qu, W. Zhou, Z. Ren, S. Du, X. Meng, G. Tian, K. Pan, G.Wang, H. Fu, Journal of
22 Materials Chemistry, **22**, 16471-16476 (2012)

- 1 [24] S. N. Tijare, M. V. Joshi, P. S. Padole, P. A. Mangrulkar, S. S. Rayalu, N. K.
2 Labhsetwar, International journal of hydrogen energy, **37**, 10451-10456 (2012)
- 3 [25] M. Ahmadipour, M. Arjmand, S. N. Q. A. Abd Aziz, S. L. Chiam, Z. A. Ahmad, & S. Y.
4 Pung, Ceramics International, **45**, 20697-20703 (2019)
- 5 [26] R. Hailili, Z. Q. Wang, X. Q. Gong, C. Wang, Applied Catalysis B: Environmental, **254**,
6 86-97 (2019)
- 7 [27] S. Kawrani, M. Boulos, D. Cornu, M. Bechelany, ChemistryOpen, **8**, 922-950 (2019)
- 8 [28] D. C. Sinclair, D. C., T. B. Adams, F. D. Morrison, A. R. West, Applied Physics
9 Letters, **80**, 2153-2155 (2002)
- 10 [29] K. Pal, A. Dey, P. P. Ray, N. E. Mordvinova, O. I. Lebedev, T. K. Mandal, M.M. Seikh
11 A. Gayen, ChemistrySelect, **3**, 1076-1087 (2018)
- 12 [30] P. R. Pansara, U. M. Meshiya, A. R. Makadiya, P. Y. Raval, K. B. Modi, P. M. G.
13 Nambissan, Ceramics International, **45**, 18599-18603 (2019)
- 14 [31] F. Moura, A. C. Cabral, L. S. R. Rocha, E. C. Aguiar, A. Z. Simões, E. Longo, Ceramics
15 International, **42**, 4837-4844 (2016)
- 16 [32] P. Thongbai, T. Yamwong, S. Maensiri, V. Amornkitbamrung, P. Chindaprasirt, Journal
17 of the American Ceramic Society, **97**, 1785-1790 (2014)
- 18 [33] S. Jin, H. Xia, Y. Zhang, J. Guo, J. Xu, Materials Letters, **61**, 1404-1407 (2007)
- 19 [34] A. K. Rai, N. K. Singh, S. K. Lee, K. D. Mandal, D. Kumar, O. Parkash, Journal of
20 alloys and compounds, **509**, 8901-8906 (2011)
- 21 [35] S. Jesurani, S. Kanagesan, T. Kalaivani, K. Ashok, Journal of Materials Science:
22 Materials in Electronics, **23**, 692-696 (2012)

- 1 [36] J. Liu, Y. Sui, C. G. Duan, W. N. Mei, R. W. Smith, J. R. Hardy, *Chemistry of*
2 *materials*, **18**, 3878-3882 (2006)
- 3 [37] D. Xu, K. He, R. Yu, X. Sun, Y. Yang, H. Xu, H. Yuan, J. Ma, *Materials Chemistry and*
4 *Physics*, **153**, 229-235 (2015)
- 5 [38] K. Pal, A. Mondal, R. Jana, P. P. Ray, A. Gayen, *Applied Surface Science*, **467**, 543-
6 553 (2019)
- 7 [39] Y. Zhu, T. Wang, W. Wang, S. Chen, E. Lichtfouse, C. Cheng C. Wang, *Environmental*
8 *Chemistry Letters*, **17**, 481-486 (2019)
- 9 [40] A. O. Turkey, M. M. Rashad, Z. I. Zaki, I. A. Ibrahim, M. Bechelany, *RSC Advances*, **5**,
10 18767-18772 (2015)
- 11 [41] J. Liu, R. W. Smith, W. N. Mei, *Chemistry of Materials*, **19**, 6020-6024 (2007)
- 12 [42] A. Lopez-Rubio, B. M. Flanagan, E. P. Gilbert, M. J. Gidley, *Biopolymers: Original*
13 *Research on Biomolecules*, **89**, 761-768 (2008)
- 14 [43] A. K. Zak, W. A. Majid, M. E. Abrishami, & R. Yousefi, *Solid State Sciences*, **13**, 251-
15 256 (2011)
- 16 [44] J. Yang, Z. Tang, H. Yin, Y. Liu, L. Wang, H. Tang, Y. Li, *Polymers*, **11**, 766 (2019)
- 17 [45] S. Jesurani, S. Kanagesan, R. Velmurugan, T. Kalavani, *Journal of Materials Science:*
18 *Materials in Electronics*, **23**, 668-674 (2012)
- 19 [46] K. Mogyorósi, K., N. Balázs, D. F. Srankó, E. Tombácz, I. Dékány, A. Oszkó, P. Sipos,
20 A. Dombi, *Applied Catalysis B: Environmental*, **96**, 577-585 (2010)
- 21 [47] S. Orrego, J. A. Cortés, R. A. C. Amoresi, A. Z. Simões, M. A. Ramírez, *Ceramics*
22 *International*, **44**, 10781-10789 (2018)

- 1 [48] P. Mishra, P. Kumar, *Ceramics International*, **41**, 2727-2734 (2015)
- 2 [49] F. Moura, A. Z. Simoes, R. C. Deus, M. R. Silva, J. A. Varela, E. Longo, *Ceramics*
- 3 *International*, **39**, 3499-3506 (2013)
- 4 [50] R. Sedghi., F. Heidari, *RSC advances*, **6**, 49459-49468 (2016)
- 5 [51] M. Mitra, S. T. Ahamed, A. Ghosh, A. Mondal, K. Kargupta, S. Ganguly, D. Banerjee,
- 6 *ACS omega*, **4**, 1623-1635 (2019)
- 7 [52] M. Ahmadipour, M. Arjmand, Z. A. Ahmad, S. Y. Pung, *Journal of Materials*
- 8 *Engineering and Performance*, 1-9 (2020)

9

10

Supplementary Files

This is a list of supplementary files associated with this preprint. Click to download.

- [RevisedElectronicSupplementaryInformation.docx](#)